An Efficient FR-1 MIMO Antenna for N78/77/48 Bands with Enhanced Isolation Using DGS

Manumula Srinubabu(✉) and Nuthakki Venkata Rajasekhar

School of Electronics Engineering (SENSE), VIT-AP University, Amaravati, Vijayawada 522237, Andhra Pradesh, India
{srinubabu.21phd7112,rajasekhar.venkata}@vitap.ac.in

Abstract. A high-efficiency, single-band microstrip patch antenna designed for the 5G-sub-6 GHz spectrum is introduced in this research. The antenna incorporates a unique defective ground structure (DGS) by integrating a rectangular cut strip to enhance its characteristics. Constructed on an FR-4 epoxy substrate using the inset feed method, the single antenna measures $15.5 \times 19.4\,\text{mm}^2$, while the proposed two-port MIMO antenna spans $52.8 \times 52.8\,\text{mm}^2$. With a moderate maximum gain of 4.1 dBi, isolation above 15 dB and radiation efficiency of 97%, this antenna operates within the frequency range of 2.5 GHz to 4.2 GHz, covering the isolation above 15 dB in the sub-6 GHz section of the N78/77/48 band in the 5G spectrum. The antenna's anticipated and observed properties affirm its suitability for 5G-NR band applications below the 6 GHz frequency range.

Keywords: 5G MIMO Antenna · DGS · Isolation · Radiation efficiency · Gain · Bandwidth

1 Introduction

It is conceivable that the technology of the 5th Generation of Communication will be implemented into mobile communication networks in the not-too-distant future. Its frequency range begins with frequencies that are lower than 6 GHz and continues all the way up to millimetre waves. The frequency band below 6 GHz, which is used for 5G, has a number of advantages, including improved coverage, accelerated data transfer speeds, and less signal loss in humid environments. [1,2]. The performance of antennas built for 5G operation in the sub-6 GHz frequency region has greatly increased, which has raised the bar for all forms of communication technology. A microstrip patch antenna is a candidate for use in 5G communication systems because of the advantages that are inherent to this kind of antenna. This is made possible by the use of a microstrip patch antenna.

N. V. Rajasekhar—Contributed equally to this work.

X. Cheng (Ed): BROADNETS 2024, LNICST 601, pp. 132–142, 2025.
https://doi.org/10.1007/978-3-031-81168-5_13

Microstrip antennas are advantageous owing to their cheap cost, low profile, flat design, conformability, lightweight, and appropriateness for arrays. In addition, they are flat and have a conformable design. In addition to that, their price is really reasonable. Microstrip antennas, which are used at low frequencies, are considered to have significant flaws in terms of gain, bandwidth, and size, all of which are considered to be significant disadvantages. [3–8]. Microstrip antennas are gaining popularity as a result of improvements in both their design and performance in recent years. Numerous strategies for boosting the performance of microstrip patch antennas have been published in [7,9–13]. These approaches may be found in a variety of different publications. These citations may be found at this location. Increases in antenna gain and bandwidth were achieved by the use of a frequency-selective surface (FSS), as described in [12]. The use of this invention resulted in the creation of a design that had a gain of 17.78 dBi at 28 GHz, a boost of 9% in bandwidth, and a radiation efficiency of 90 percent. In this article, the construction and modelling of a wideband antenna are discussed. Based on the observations, it seems that a bandwidth ranging from 5.50 to 7.25 GHz was successfully achieved. In [9], FSS was used to broaden the bandwidth of the antenna, which ultimately resulted in a gain of 9.4 dBi. The antenna has an extremely broad frequency range, spanning from 3.1 GHz all the way up to 18.6 GHz. In addition to that, the ratio of this antenna's front lobe to its rear lobe is a high 10 dB over the whole of the UWB (ultra-wideband) band. Following the use of DGS in antenna arrays in [10], the 22 array was designed with a 12 dB increase in radiation between the co-pole and cross-pole radiation. This step was taken after going through and looking at the arrays there. When the DGS and the reflecting plate were applied to the antenna, the results were reported in [13] as a four-element linear array with gains of 9.02 dB and directivities of 12.81 dB, respectively. This was accomplished. A single-layer, single-probe-fed wideband antenna is described in this [14]. The antenna has one layer. A rectangular patch with a parasitic pattern in the form of a U was developed first, before the construction of the radiating patch. The antenna that was created as a consequence emitted electromagnetic waves at frequencies ranging from 4.82 GHz to 6.26 GHz, 5.25 GHz to 5.35 GHz, and 5.725 GHz to 5.875 GHz. Slots have been thoughtfully cut out of the ground plane of the antenna in order to provide room for the DGS component of the design. These slots have an inductive influence on the circuit, and they also have a capacitive impact on the circuit. The total performance of the antenna may be improved by optimizing the circuit, which can be accomplished by adjusting both the size of the slot and its position [15]. To ensure that the circuit works as efficiently as it possibly can, the slot sizes and locations are given careful consideration. When it is adequately calibrated, the impedance that the DGS design contributes to the circuit may be used to reduce the size of the antenna, increase its bandwidth, and boost its gain [16–18]. This is only possible if the impedance is properly tuned for different scenarios. Thus, it can be observed that wide bandwidth antennas must be modelled to improve performance under real-time use cases. To perform this task, the next section proposes the design of a high bandwidth n78 band

FR-1 antenna with isolation enhancements via DGS. The model was simulated and results were compared with standard techniques, under real-time scenarios.

2 Antenna Design Details

The given N78/48/77 band FR (frequency range)-1 antenna uses a technique founded on a transmission model to calculate an approximate antenna size. The antenna operates at a frequency of 3.55 GHz and is constructed on a substrate made of FR-4 epoxy with a dielectric constant of 4.4.

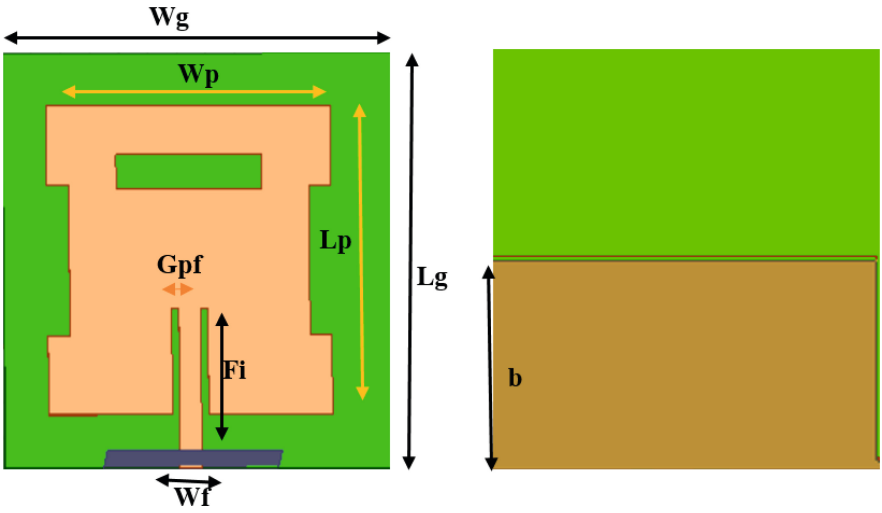

Fig. 1. Single monopole antenna front and rear view

The timing of its execution is also detailed. The recommended form of the FR1 antenna for the N78/48/77 band is seen in Figs. 1 and 2, which may be found here. This illustration clearly demonstrates the usage of DGS in the design of the provided antenna from above to enhance the antenna's qualities. You can tell by looking at the graph. The microstrip antenna, which does not use DGS, is responsible for the limited bandwidth. In order to permit broad operation in the sub-6 GHz frequency range, the ground plane of the FR-1 antenna has to be modified for the N78/48/77 band. As a means of improving the antenna's gain, a triangular strip was inserted into the ground plane. To do this, the strip was laid flat on the ground. The inset feed strategy, matched to a 50-ohm feeding impedance, has been chosen as the optimal feeding technique for the projected N78/48/77 band FR-1 antenna. This decision was made after much deliberation over other diet plans. After the antenna has been optimized, a reflective plate is attached to it and placed only two millimetres above the ground plane. This process is carried out to improve the antenna's radiation.

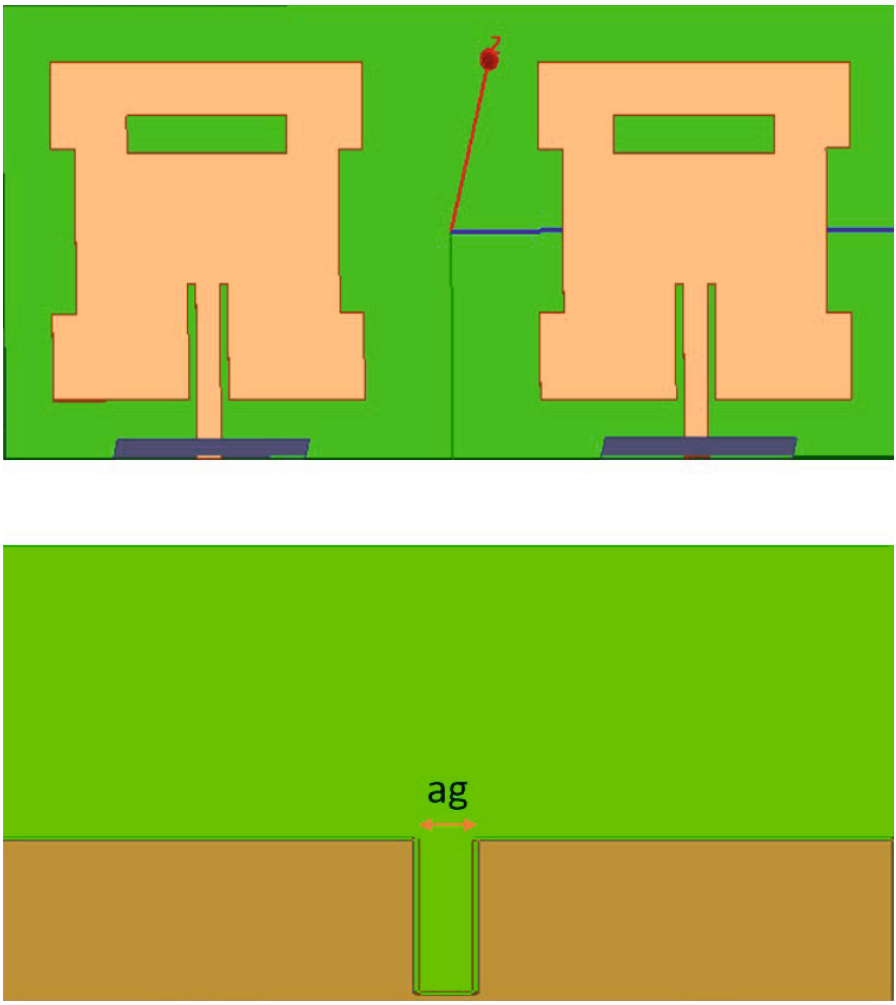

Fig. 2. Design of the proposed antenna front and rear view of the patch with element gap = 32.5 mm

The copper coating on top of the reflecting plate has been etched away (i.e., single layer sheet). The copper reflecting surface on the underside of the plate will remain in place and no copper will be added to the top. The antenna's side lobes may be focused and improved with the help of the reflecting plate, which acts as a reflector. The copper reflecting surface at the plate's underside is not removed since it serves an essential purpose in the reflector. The N78/48/77 band FR1 antenna has been proposed as an alternative since it operates in a frequency range appropriate for 5G communications while still being below 6 GHz. Research into the proposed FR-1 antenna was grounded on equations derived from the transmission model. The proposed antenna may be modelled

as a lumped circuit, with resistors, inductors, and capacitors standing in for the patch's inherent impedance, respectively. However, the antenna's ground plane, which has an etched triangular DGS pattern, may be replaced with inductors and capacitors if necessary. The term "ground plane of the antenna" is used to describe inductance even though other resistors, inductors, and capacitors also show the inductance introduced by the ground plane of the antenna. The separation is done by placing antennas at a distance of 32.5 mm, which assists in dual port feeding operations. Through the use of Eq. 1, the equivalent impedance may be precisely determined.

$$Z_{in} = Z_{dgs\|} Z_p \parallel Z_{ref}. \tag{1}$$

Following the application of the patch, the impedance is denoted by Z_p. Z_{dgs} is used to describe the impedance that DGS induces. Z_{ref} is used to represent the impedance that is brought on by the reflecting plate. In this instance, isolation is accomplished via the use of both polarization diversity and straightforward DGS. Application of rectangular-shaped microstrip line feed configuration achieves impedance matching operations. The width of the rectangular patch may be determined using Eq. 2,

$$W = \frac{c}{2f_r}\sqrt{\frac{2}{\varepsilon_r + 1}}. \tag{2}$$

which is based on the transmission line model equations found in Eq. 3, In this expression, the constants c (light speed), f_r (resonant frequency), and r (substrate dielectric constant) all have their own characteristics. The height of the substrate is denoted by h in this context h is 1.6 mm, the dielectric constant, is denoted by $\varepsilon_r = 4.4$, and the loss tangent is denoted by $\tan\delta = 0.02$. In addition to this, we determined that the resonance frequency, denoted by f_r, is 3.55 GHz. We can figure out the dimensions of the patch by using the formulas from Eqs. 5, and we find that its length is 15.5 mm and its width is 19.4 mm.

$$\varepsilon_{reff} = \frac{\varepsilon_r + 1}{2} + \frac{\varepsilon_r - 1}{2\sqrt{1 + \frac{12h}{w}}}. \tag{3}$$

If you wish to maintain the square shape of the Patch while increasing the amount of rotation in the circular field, keep the width equal to the length. Because of this, the antenna will have a lower frequency at which it resonates.

$$L = L_{eff} - 2\Delta L = \frac{c}{2 * f_r\sqrt{\varepsilon_{eff}}} - 2\Delta L. \tag{4}$$

$$\Delta L = \frac{0.412 * h(\varepsilon_{reff} + 0.3)(\frac{w}{h} + 0.264)}{(\varepsilon_{reff} - 0.258)(\frac{w}{h} + 0.8)} \tag{5}$$

In order to achieve a frequency of 3.55 GHz, it was necessary to raise the length to 52.8 mm; conversely, decreasing the patch size led to an increase in operating frequency. Achieving the necessary axial ratio required some trial and error to identify the appropriate degree of chamfering to apply to the edges.

In order to make room for the printed circuit board (PCB), a hole was drilled through the middle of the board. The dimensions of the cut were also adjusted to ensure the lowest possible S_{21} between the antennas while they are both broadcasting and receiving on the same frequency. This is accomplished by fine-tuning the size of the cut. It is possible to get a decoupling of −15 dB in conditions when everything goes well. In the next section of this text, we are going to analyse the results that arise from following these designs.

3 Results and Comparative Analysis

The substrate of this antenna is made of FR-4, which has a significant loss (measured as a tangent, or tan), which comes in at 0.02. You may get some FR-4 at a minimal cost and acquire some with little to no work on your part. The lossy of the substrate has no effect on the performance of the antenna. The simulation is carried out with the help of an HFSS toolkit that is available for purchase.

The findings of the study on the design procedure of the N78/48/77 band FR-1 antenna are presented and spoken about in this article. When there is just the DGS present, the antenna is referred to as an antenna with DGS (ADGS), and when there is neither the DGS nor the reflecting plate present, the antenna is referred to as a plane antenna (PA). The dielectric ground plane and the reflecting plate are the components that make up the entire antenna, also known as the N78/48/77 band FR-1 antenna. When it comes to the radiation properties, the FR1 antenna for the n78 band performs superiorly to both ADGS and PA. The reflective plate that is secured to the rear of the n78 band FR1 antenna has been simulated, optimized, and fine-tuned to the point where it has been found that a distance of 1.6 mm is the most effective placement for it. A substrate made of FR-4 with just one side reflective is used for the reflecting surface The information on the plate's thickness may be found in Table 1,

Table 1. Design parameters for the given antenna configuration

Parameters	Dimensions (mm)
Wg	15.5
Lg	19.4
Wp	12.35
Lp	10.5
h	1.6
Fi	4.5
Wf	2.95
Gpf	0.8
ag	1.5
b	9.4

By minimizing both the antenna and the back lobe, the plate enables the antenna to radiate in a more focused manner. The antenna's gain is increased because of an inventive triangular plate that was placed on the ground plane. This plate also contributes to the design's already impressively broad bandwidth. A highly restricted antenna range would result in the absence of the triangular slot on the antenna. It's possible that we can increase the antenna's bandwidth even more if we cut a triangular slit in the ground plane and then optimize it. To ensure that the design produces a satisfactory response, the ideal dimensions of the antenna and the triangular plate utilized in the construction are detailed in Table 1. The computed reflection coefficients for the three different experimental settings are shown in Fig. 3,

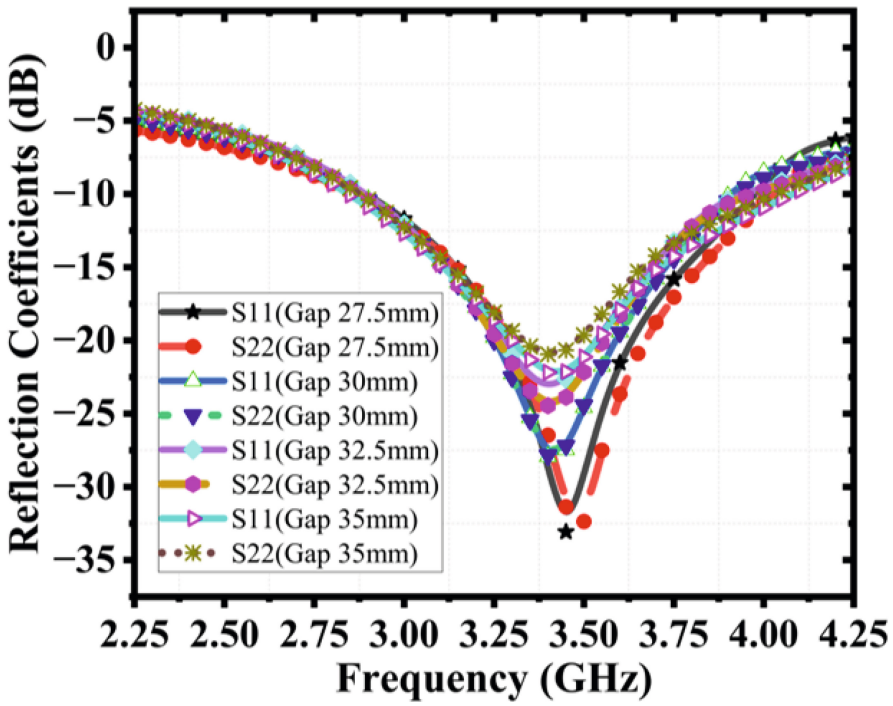

Fig. 3. Simulated results of the proposed 3-port MIMO antenna with different element gaps

In comparison, the PA and ADGS antennas have minimum values of S_{21} −15 dB and −22 dB, respectively, for their reflection coefficients, while the FR1 antenna is for the n78/48/77 band. The frequency range of the proposed n78 band FR1 antenna is 2.521 GHz to 4.2784 GHz, which proves without a reasonable doubt that it has a single band in the frequency that is lower than 6 GHz as observed from Figs. 3, 4 and 5 as follows,

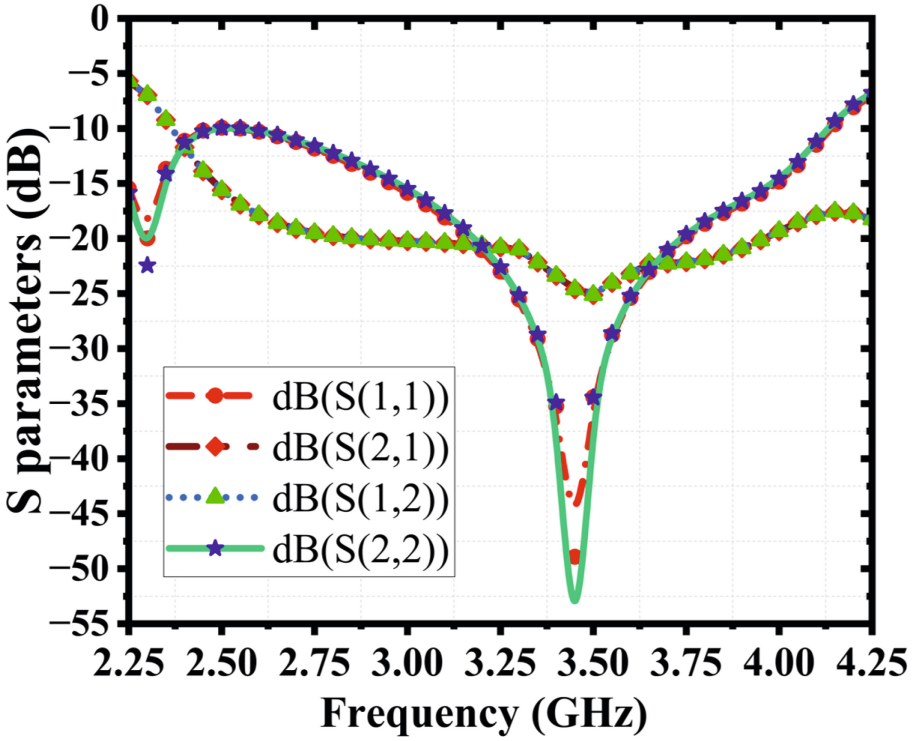

Fig. 4. Simulated S_{xx} results of the proposed MIMO designs

Table 2. Results of the proposed antenna

Ref.	Size	Op. Freq. (GHz)	BW Axial Ratio (%, Hz)	Gain (dBi)
[2]	175 × 47 × 1.7	1.75, 1.85, 1.95, 2.15, 2.6		2.1, −1.7, 1.9, 3.2, 4.8
[4]	58 × 40 × 1.6	1.51–3.69/4.67–5.25/5.78–5.96	83.8/11.69/3.06	5.2/4.8/5
[8]	R = 15 mm	4.74–6.79 GHz	35.55	4.2 dbi
[9]	70 × 30 × 1.6	770–1000 MHz/1.7–3.78 GHz	240 MHZ/2400 MHZ	3.54/5.89/3.52
[10]	51 × 52 × 1.6	1.17645 GHz/2.320–2.34 5 GHz/1.9 GHz	12–25 MHZ	3/6.5
[13]	87.5 × 61 × 1.6	1.8–2.9/3.4–4.6/5–5.6		2.58–3.34 dbi
[7]	75 × 75	1.575 /3.71/ 5.9 GHz	16.8 MHz/ 77 MHz/154 MHz	5.5 dbi/8 dbi/9 dbi
[1]	55 × 40 × 3	1.78–5.28/5.62–6.08	99.15/7.83	7
Our	52.8 × 52.8	2.5–4.278	2500–4278 MHz	Nearly 4.1 dBi

In the following table, the findings of the suggested model are contrasted with those of the methodologies that are currently in use. Similarly, isolation results can be observed in Fig. 4, which showcases DGS and without DGS outputs. Based on this, it can be observed that the proposed model is able to improve the isolation efficiency for different use cases. Thus, the proposed model of the antenna showcases good results and can be used for real-time use cases (Table 2).

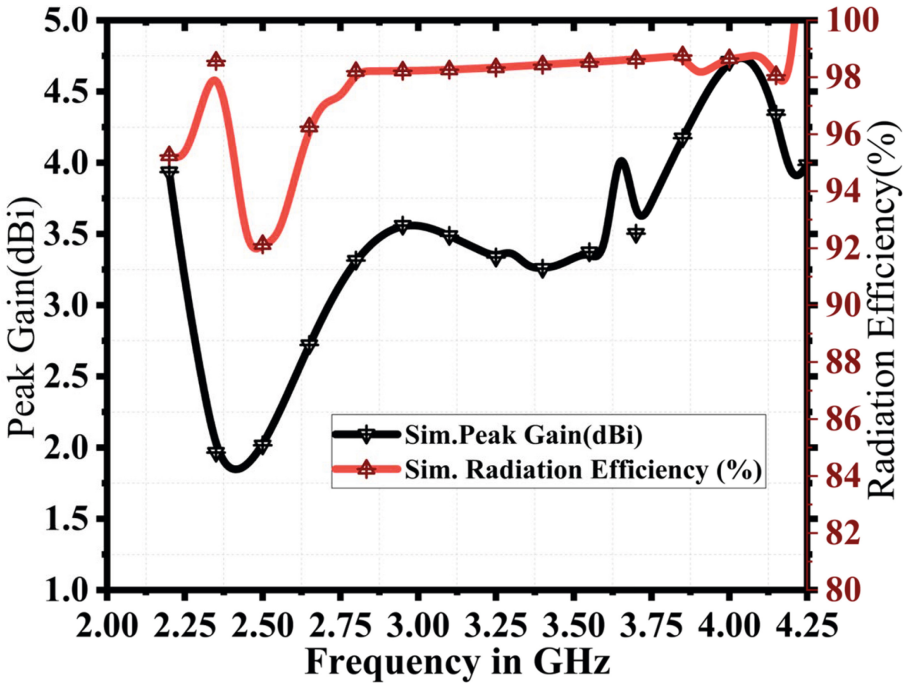

Fig. 5. Simulated radiation efficiency and gain results of the proposed MIMO designs

4 Conclusion and Future Scope

A small, rectangular microstrip patch antenna with high gain across a wide frequency range has been released, and it has been designed specifically for use in 5G applications operating at frequencies lower than 6 GHz. When running the simulations and trying to get the designs as good as they could be, we used a commercial EM tool called HFSS. The suggested single antenna has a substrate that is 15.4 mm by 19.4 mm, its best gain is just 4.1 dB, and its radiation efficiency is 97%. This effective antenna design, which has a frequency range that extends from 2.5 GHz to 4.2785 GHz and beyond, is able to cover the sub-6 GHz region of the 5G spectrum, which spans from 3 GHz to 4 GHz. A satisfactory fabrication and testing process has been completed for the FR-1 N78/48/77 band antenna. The findings obtained from both the simulation and the measurements are consistent with one another to a satisfactory degree. According to the technical specifications of the antenna, it has been shown that the proposed tiny N78/77/48 band FR-1 antenna is capable of handling 5G communications at frequencies lower than 6 GHz. Utilizing computer models that are biologically inspired will make it possible to simulate, in the future, the

modelled antenna on a variety of substrates; this will allow for the adjustment of its size as well as the increase of its overall efficiency levels.

References

1. Satyanarayana, B., Srivastava, S.K., Meshram, M. K.: Compact 8-port coupled-fed MIMO antenna array for sub-6 GHz 5G smartphone terminals. In: IEEE MTT-S International Microwave and RF Conference (IMARC), pp. 1–4 (2021). https://doi.org/10.1109/IMaRC49196.2021.9714563
2. Kulkarni, J., Chitre, A., Kulkarni, N., Kulkarni, S., Talware, R.: Design and analysis of compact 2D MIMO sub-6 GHz 5G flexible antenna. In: 2021 IEEE Madras Section Conference (MASCON), pp. 1–5 (2021). https://doi.org/10.1109/MASCON51689.2021.9563492
3. Chaimool, S., Sangwijit, B., Pukna, P., Rakluea, C.: A dual-band dual-polarized MIMO antenna for 700 MHz and sub-6 GHz 5G systems. In: 2020 International Symposium on Antennas and Propagation (ISAP), pp. 103–104. IEEE (2021)
4. Kumari, P., Kumari, T., Suman, K.K., Gangwar, R.K., Chaudhary, R.K.: A circularly polarized sub-6 GHz MIMO antenna for 5G applications. In: 2022 IEEE International Symposium on Antennas and Propagation and USNC-URSI Radio Science Meeting (AP-S/URSI), pp. 1186–1187. IEEE (2022)
5. Zheng, Z., Ntawangaheza, J., Sun, L.: Wideband MIMO antenna system for sub-6 GHz cell phone. In: 2021 International Conference on Electronics, Circuits and Information Engineering (ECIE), pp. 1–5. IEEE (2021)
6. Rafique, U., et al.: Uni-planar MIMO antenna for sub-6 GHz 5G mobile phone applications. Appl. Sci. **12**(8), 3746 (2022)
7. Chen, Y.-R., Chen, W.-S.: Design of MIMO WLAN 2.4/5.2/5.8 and 5G sub-6 GHz antennas for laptop computer applications. In: 2020 International Workshop on Electromagnetics: Applications and Student Innovation Competition (iWEM), pp. 1–2. IEEE (2020)
8. Patnaik, P., Sarkar, D., Saha, C.: A multi-band 5G antenna for smart phones operating at sub-6 GHz frequencies. In: 2020 International Symposium on Antennas & Propagation (APSYM), pp. 32–35. IEEE (2020)
9. Supreeyatitikul, N., Phungasem, A., Aeimopas, P.: Design of wideband sub-6 GHz 5G MIMO antenna with isolation enhancement using an MTM-inspired resonators. In: 2021 Joint International Conference on Digital Arts, Media and Technology with ECTI Northern Section Conference on Electrical, Electronics, Computer and Telecommunication Engineering, pp. 206–209. IEEE (2021)
10. Shameena, V., Anila, P., Mohanan, P.: A compact four-element self decoupled MIMO antenna for sub-6 GHz 5D applications. In: 2021 IEEE International Symposium on Antennas and Propagation and USNC-URSI Radio Science Meeting (APS/URSI), pp. 1233–1234. IEEE (2021)
11. Manirathnam, C., Ghosh, S., Swati, M.: A compact, two-port MIMO antenna for mm-wave 5G application. In: 2022 IEEE 11th International Conference on Communication Systems and Network Technologies (CSNT), pp. 22–25. IEEE (2022)
12. Alam, T., Cheffena, M.: Four-port multiband MIMO filtenna with an isolation filter for sub-6 GHz 5G applications. In: 2021 IEEE MTT-S International Microwave Filter Workshop (IMFW), pp. 281–283. IEEE (2021)

13. Chandra, R., Sarkar, D., Ganguly, D., Saha, C., Siddiqui, J.Y., Antar, Y.M.: Design of NFRP based sir-loaded two element MIMO antenna system for 28/38 GHz sub mm-wave 5G applications. In: 2020 IEEE 3rd 5G World Forum (5GWF), pp. 514–518. IEEE (2020)
14. Saxena, S., Dwari, S., Kanaujia, B.K.: Design of 4 (n+ 1) element dual-CP massive MIMO antenna for 5G systems operating in sub-6 GHz band. In: 2020 Third International Conference on Advances in Electronics, Computers and Communications (ICAECC), pp. 1–4. IEEE (2020)
15. Parchin, N.O., Al-Yasir, Y.I., Abdulkhaleq, A.M., Basherlou, H.J., Ullah, A., Abd-Alhameed, R.A.: A new broadband MIMO antenna system for sub 6 GHz 5G cellular communications. In: 2020 14th European Conference on Antennas and Propagation (EuCAP), pp. 1–4. IEEE (2020)
16. Molins-Benlliure, J., Cabedo-Fabrés, M., Antonino-Daviu, E., Ferrando-Bataller, M.: Eight-port wideband MIMO antenna for sub-6 GHz 5G base stations. In: 2021 IEEE International Symposium on Antennas and Propagation and USNC-URSI Radio Science Meeting (APS/URSI), pp. 839–840. IEEE (2021)
17. Babu, S.S., Patre, S.R.: Meandered-line folded antenna for sub-6 GHz supported MIMO system. In: 2022 3rd International Conference for Emerging Technology (INCET), pp. 1–4. IEEE (2022)
18. Hussain, R., Khan, M.U., Almajali, E., Sharawi, M.S.: An integrated MIMO antenna for sub-6 GHz and millimeter-wave bands for 5G applications. In: 2020 IEEE International Symposium on Antennas and Propagation and North American Radio Science Meeting, pp. 1293–1294. IEEE (2020)